NASA/CR-20250003216

Uncertainty Analysis of the NASA Glenn 6- by 9-Foot Icing Research Tunnel 2024 Characterization Test

Pamela Poljak and Laura Hux
Amentum/TFOME II, Cleveland, Ohio

April 2025

NASA STI Program . . . in Profile

Since its founding, NASA has been dedicated to the advancement of aeronautics and space science. The NASA scientific and technical information (STI) program plays a key part in helping NASA maintain this important role.

The NASA STI program operates under the auspices of the Agency Chief Information Officer. It collects, organizes, provides for archiving, and disseminates NASA's STI. The NASA STI program provides access to the NTRS Registered and its public interface, the NASA Technical Reports Server, thus providing one of the largest collections of aeronautical and space science STI in the world. Results are published in both non-NASA channels and by NASA in the NASA STI Report Series, which includes the following report types:

- TECHNICAL PUBLICATION.
  Reports of completed research or a major significant phase of research that present the results of NASA programs and include extensive data or theoretical analysis. Includes compilations of significant scientific and technical data and information deemed to be of continuing reference value. NASA counterpart of peer-reviewed formal professional papers but has less stringent limitations on manuscript length and extent of graphic presentations.

- TECHNICAL MEMORANDUM.
  Scientific and technical findings that are preliminary or of specialized interest, e.g., quick release reports, working papers, and bibliographies that contain minimal annotation. Does not contain extensive analysis.

- CONTRACTOR REPORT.
  Scientific and technical findings by NASA-sponsored contractors and grantees.

- CONFERENCE PUBLICATION.
  Collected papers from scientific and technical conferences, symposia, seminars, or other meetings sponsored or cosponsored by NASA.

- SPECIAL PUBLICATION.
  Scientific, technical, or historical information from NASA programs, projects, and missions, often concerned with subjects having substantial public interest.

- TECHNICAL TRANSLATION.
  English-language translations of foreign scientific and technical material pertinent to NASA's mission.

Specialized services also include organizing and publishing research results, distributing specialized research announcements and feeds, providing information desk and personal search support, and enabling data exchange services.

For more information about the NASA STI program, see the following:

- Access the NASA STI program home page at http://www.sti.nasa.gov

NASA/CR-20250003216

Uncertainty Analysis of the NASA Glenn 6- by 9-Foot Icing Research Tunnel 2024 Characterization Test

Pamela Poljak and Laura Hux
Amentum/TFOME II, Cleveland, Ohio

Prepared under Contract NNC15BA02B

National Aeronautics and
Space Administration

Glenn Research Center
Cleveland, Ohio 44135

April 2025

Acknowledgments

This work was sponsored by the Aerosciences Evaluation and
Test Capabilities (AETC) Portfolio at the NASA Glenn Research Center.

Level of Review: This material has been technically reviewed by NASA expert reviewer(s).

This report is available in electronic form at https://www.sti.nasa.gov/ and https://ntrs.nasa.gov/

NASA STI Program/Mail Stop 050
NASA Langley Research Center
Hampton, VA 23681-2199

Contents

List of Figures

List of Tables

Uncertainty Analysis of the NASA Glenn 6- by 9-Foot Icing Research Tunnel 2024 Characterization Test

Pamela Poljak
Laura Hux
Amentum/TFOME II
Cleveland, Ohio 44135

1 Abstract

This Contractor Report presents methods and results of a measurement uncertainty analysis that was performed for the 6- by 9-Foot Icing Research Tunnel (IRT) located at the NASA Glenn Research Center. The systematic uncertainty analysis is based on data collected during a facility characterization test conducted in 2024. The random uncertainty analysis is based on data collected in 2021, 2023, 2024 and 2025. The statistical methods and engineering judgments used to estimate elemental uncertainties are described in this report. The Monte Carlo method was used to propagate systematic components of uncertainty through the data reduction process in order to quantify the uncertainty in variables of interest (VOIs). A description of the Monte Carlo method as applied for this analysis is provided.

Nomenclature

Acronyms and Abbreviations

AoA	angle of attack
CE–12	NASA Glenn Research Center Free-Jet Probe Characterization Facility
ESP	electronic scanning pressure
IRT	Icing Research Tunnel
MANTUS	measurement analysis tool for uncertainty in systems
MCM	Monte Carlo Method
MUA	measurement uncertainty analysis
PCU	pressure control unit
RMSE	root mean square error
RTD	resistance temperature detector
TSM	Taylor Series Method
VOI	variable of interest

Calculated Variables

$APSC$	5-hole flow angle probe average static pressure of 7 core probes, psia
$APTC$	5-hole flow angle probe average total pressure of 7 core probes, psia
$ATTARRCC25$	average of 25 center 2D RTD array temperature measurements, thermal recovery corrected, °C
CA	5-hole flow angle probe pressure coefficient, psia
CB	5-hole flow angle probe pressure coefficient, psia
CM	5-hole flow angle probe pressure coefficient, psia
Co	5-hole flow angle probe total pressure correction factor, psia
MFJ	CE–12 free-jet Mach number [2D RTD array probe calibration]
MTS	test section Mach number
$PAIRAVG$	average spray bar air pressure, psig
$PRATBM$	bellmouth pressure ratio, PSBM/PTBM, psia
$PSBM$	average bellmouth static pressure, psia
$PSTS$	test section static pressure, psia
$PTBM$	average bellmouth total pressure, psia
$PTTS$	test section total pressure, psia
$TSTS$	test section static temperature, °C
$TTDC$	average D-corner total temperature, °C

$TTDELTA$	difference between D-corner temperature and corrected test section temperature, °C
$TTTS$	test section total temperature, °C
UTS	test section airspeed, knots

Measured Inputs

D_RTD(11-83)	D-corner RTD measured temperatures (24 total), °C
$ESPREF$	barometric reference pressure, psia
$P1$	5-hole flow angle probe Port 1 total pressure, psia
$P2 - P5$	5-hole flow angle probe flow angle pressure Ports 2 through 5, psia
$P6$	5-hole flow angle probe static pressure, psia
Ps	Aeroprobe 5-hole flow angle probe calibration, facility atmospheric pressure, Absolute Torr
$PSBMN$	bellmouth static pressure north, psia
$PSBMS$	bellmouth static pressure south, psia
$PSFJ$	CE–12 free-jet static pressure [2D RTD array probe calibration], psia
Pt	Aeroprobe 5-hole flow angle probe calibration, facility total pressure, Torr
$PTBMN$	bellmouth total tressure north, psia
$PTBMS$	bellmouth total pressure south, psia
$PTFJ$	CE–12 free-jet total pressure [2D RTD array probe calibration], psia
TT_RTD(11-49)	2D RTD array probe temperature measurements [2D RTD array probe calibration] (49 total), °F
$TTARRC$(11-49)	2D RTD array temperature measurements (49 total), °C
$TTFJ$	CE–12 free-jet total temperature [2D RTD array probe calibration], °F
$WDPF$(1-10)	spray bar measured pressures (10 total), psig

Subscripts

avg	refers to the average of a data set
AP	refers to 5-hole flow angle probe characterization measured input
cal	refers to 5-hole flow angle probe characterization process
$model$	refers to curve fit model for the variable of interest
x	refers to variable x

Symbols

$2D$	two dimensional
γ	ratio of specific heats
B	expanded systematic uncertainty
b	elemental standard systematic uncertainty

k	coverage factor
R	universal gas constant, N*m/(kg*kelvin)
s	elemental standard random uncertainty
$sigma$	the standard deviation of a population

2 Introduction

This Contractor Report details the measurement uncertainty analysis (MUA) performed in 2025 for the NASA Glenn 6- by 9-Foot Icing Research Tunnel (IRT). Data used for the systematic uncertainty analysis were obtained during a series of characterization test runs conducted in the IRT in 2024. Data used for the random uncertainty analysis were collected in 2021, 2023, 2024, and 2025. A detailed description of the characterization test procedures can be found in the characterization test report, *Full Aerothermal Characterization of the NASA Glenn Research Center 6- by 9-Foot Icing Research Tunnel (2023 Test)* (Ref. [1]).

The objective was to determine the uncertainty in the primary test section VOIs: static and total pressure, static and total temperature, Mach number and air speed. In addition to determining the listed test section uncertainties, the elemental contributors that drive these uncertainties were also identified.

The document provides background information on the facility, including a brief description of the facility and how it operates, as well as the calibration procedure used to define the test section conditions. The uncertainty sources considered in this analysis are defined, and a description of the ways in which these uncertainties were propagated is given. A summary of the results is presented and discussed.

3 Overview

3.1 Description of the 6- by 9-Foot Icing Research Tunnel

The IRT is a closed loop atmospheric wind tunnel illustrated in Figure 1. The facility test section is 6-ft high, 9-ft wide, and 20-ft long, with no divergence along any of the test section surfaces. Airflow is driven by a 25-ft-diameter, 12-blade fan powered by a 5000-horsepower electric motor with an operating range from 25 knots up to 300 knots. A heat exchanger located in the C-D leg of the tunnel loop allows for total temperature settings as low as -40 °C. A set of 10 horizontally oriented spray bars, located in the settling chamber, prior to the bellmouth inlet upstream of the test section, inject atomized water into the airflow to create specific icing cloud conditions. A turntable, located in the test section, is used to rotate mounted hardware to different angles of attack (AoA) during testing.

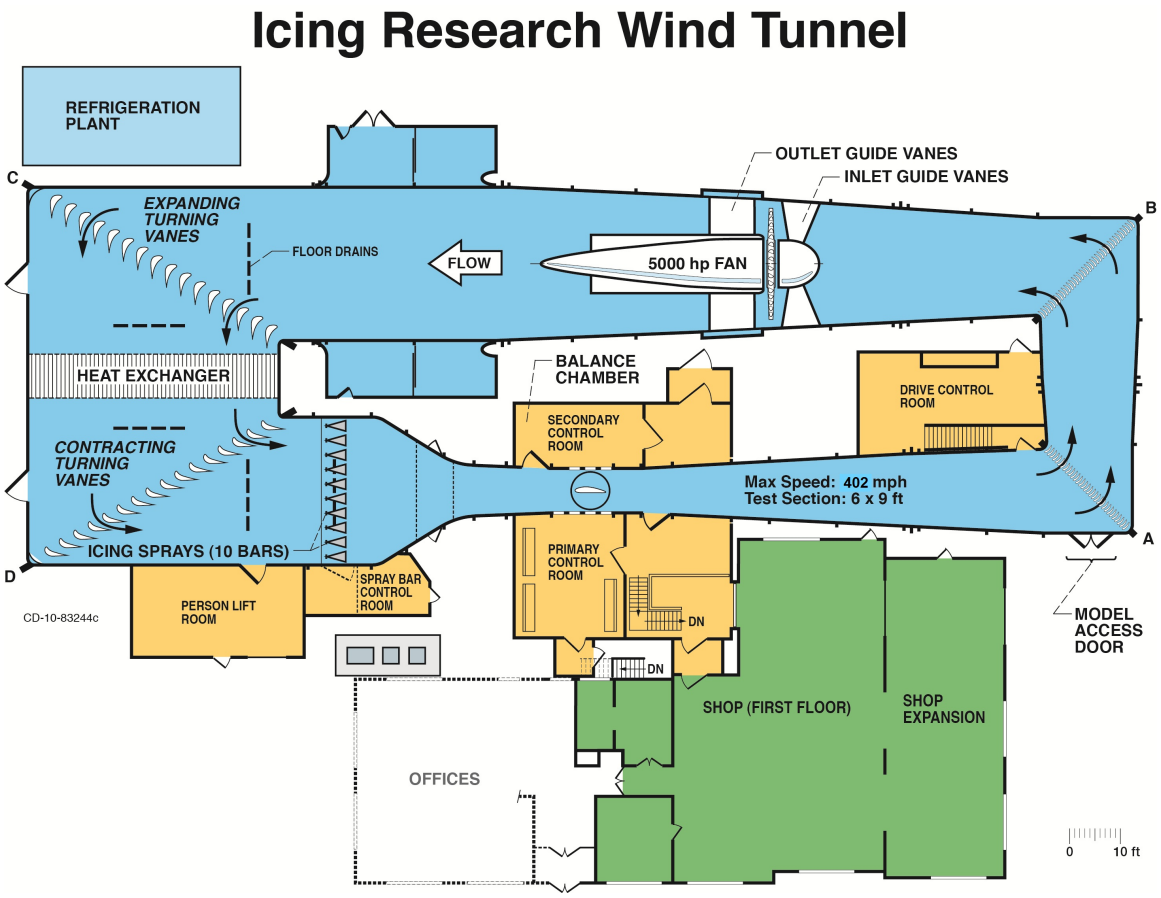

Figure 1. Schematic of 6- by 9-Foot Icing Research Tunnel Facility.

3.2 Characterization Test

Full characterization includes collection of aerothermal calibration data over the entire operating range of the IRT, as well as a complete mapping of the IRT flow quality at one cross section of the test section, typically the centerline of the turntable. Ideally, a full characterization is conducted every five years or following a major facility modification. The full characterization provides all of the information needed to develop the aerothermal calibration relationships for the facility and provides extensive detailed information on the aerothermal flow quality characteristics of the test section.

4 Instrumentation

During an aerothermal characterization test, facility operating conditions are set by controlling the airspeed, spray bar air pressure, and air temperature. Data collected using facility and aerothermal calibration instrumentation are then used to develop regression models to predict test section conditions as a function of facility instrumentation measurements.

4.1 Facility Instrumentation

Instrumentation critical to facility operations are located at the D-corner turning vanes, spray bar array manifolds, and in the bellmouth upstream of the test section as shown in Figure 1.

Air temperature is measured using 24 resistance temperature detectors (RTDs) located on the leading edge of the D-corner turning vanes. A schematic of the RTD probe array layout is shown in Figure 2. Spray bar air pressure is measured by 10 100-psig pressure transducers, one on each of the 10 spray bars. Bellmouth static and total pressure are measured by two pitot-static probes, one mounted on the north wall and the other on the south wall near the exit of the bellmouth contraction as shown in Figure 3. The pitot-static probes are plumbed to a ±5-psid module on a Netscanner 9816 electronic scanning pressure (ESP) system. Barometric reference pressure is measured with a 23-psia Netscanner 9034 pressure control unit (PCU). The barometric reference pressure is combined with the differential pressures to obtain absolute pressures.

A list of critical facility instrumentation is shown in Table I. Table II shows a list of critical calculated VOIs.

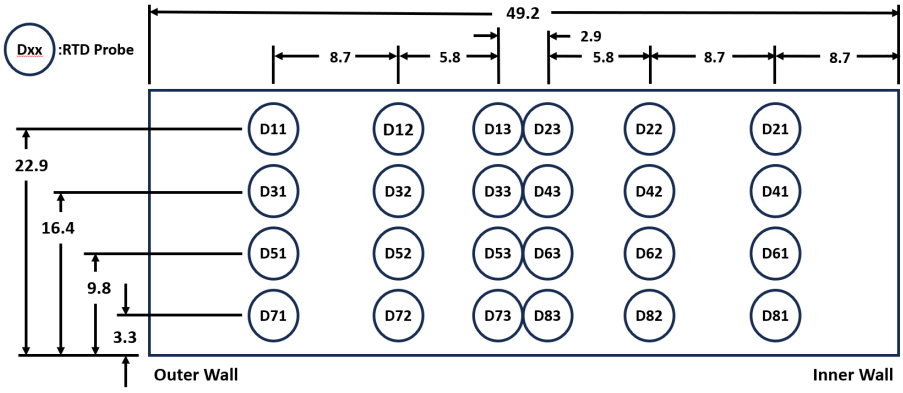

Figure 2. D-corner RTD probe array layout. All dimensions are in feet.

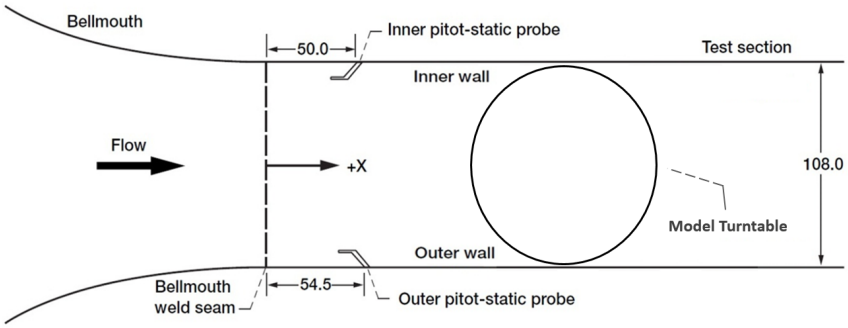

Figure 3. Icing Research Tunnel bellmouth and test section (top view). All dimensions are in inches.

TABLE I. CRITICAL FACILITY INSTRUMENTATION MEASUREMENTS

Variable Name	Description	Units	Quanitity	Measurement System
$ESPREF$	Barometric reference pressure	psia	1	ESP PCU, 0 to 23 psia
$PTBMN, PTBMS$	Bellmouth total pressure	psia	2	ESP, ±5-psid module, ESP PCU, 0 to 23 psia
$PSBMN, PSBMS$	Bellmouth static pressure	psia	2	ESP, ±5-psid module, ESP PCU, 0 to 23 psia
$TCD[11-83]$	D-corner temperature	°C	24	Accutech RTD
$WDPF[1-10]$	Spray bar pressure	psig	10	Honeywell pressure transducer, 100 psig

TABLE II. CRITICAL CALCULATED VARIABLES OF INTEREST

Variable Name	Description	$f(x)$
$PTBM$	Average total pressure in bellmouth	$f(PTBMN, PTBMS)$
$PSBM$	Average static pressure in bellmouth	$f(PSBMN, PSBMS)$
$PAIRAVG$	Average spray bar air pressure	$f(WDPF(1-10))$
$PRATBM$	Ratio of static to total pressure in bellmouth	$f(PTBM, PSBM)$
$TTDC$	Average total temperature in D-corner	$f(TCD(11-83))$
$PSTS$	Static pressure in test section	$f(PSTS_{model}, PRATBM, PSBM)$
$PTTS$	Total pressure in test section	$f(PTTS_{model}, PRATBM, PAIRAVG, PTBM)$
$TTTS$	Total temperature in test section	$f(TTTS_{models}(Low \text{ or } HighSpeed), PRATBM, PAIRAVG, TTDC)$
MTS	Mach number in test section	$f(PSTS, PTTS, \gamma)$
$TSTS$	Static temperature in test section	$f(TTTS, MTS, \gamma)$
UTS	Airspeed in test section	$f(TSTS, MTS, \gamma, R)$

4.2 Pressure Calibration Instrumentation

4.2.1 6-ft Quick-Check Rake

The IRT 6-ft quick-check rake was used to collect test section data during the pressure calibration portion of the characterization tests. In the fully populated configuration, the rake is instrumented with 11, 5-hole flow angle probes, described in Section 4.2.2. Figure 4 shows a photograph of the rake mounted on the centerline of the test section. The 5-hole flow angle probes are plumbed to a ±5-psid module on a Netscanner 9816 ESP system. The barometric reference pressure is combined with the differential pressures to obtain absolute pressures.

Figure 4. Icing Research Tunnel 6-ft quick-check rake.

4.2.2 5-Hole Flow Angle Probes

The 5-hole flow angle probes used on the 6-ft quick-check rake were fabricated and calibrated by Aeroprobe Corporation. A description of the calibration process is provided in Section 5.3. These probes were used to measure static pressure, total pressure, and flow angularity in the test section of the IRT during the pressure calibration portion of the characterization test. Each probe was heated to prevent ice buildup on the pressure ports during testing. The probes have a total of five pressure ports distributed on a hemispherical tip and a static pressure ring 3.9 inches downstream of the tip. Total pressure $P1$ is sensed by the center port on the head. Flow angle pressures $P2$, $P3$, $P4$, and $P5$ are sensed by the circumferential ports on the probe head. The static pressure ring tap holes are manifolded into a single pressure measurement, $P6$, as shown in Figure 5. Critical instrumentation measurements and 5-hole flow angle probe calibration variables are shown in Tables III and IV.

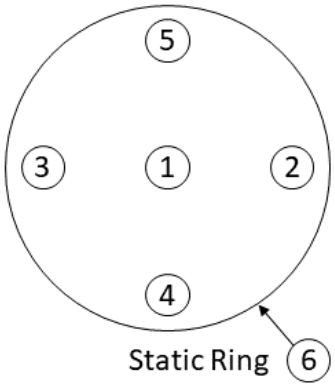

Figure 5. Aeroprobe Corporation 5-hole flow angle probe (forward looking aft).

TABLE III. CRITICAL 5-HOLE FLOW ANGLE PROBE INSTRUMENTATION MEASUREMENTS

Variable Name	Description	Measurement System
$P1$	Total pressure measured at Port 1 of 5-hole probe	ESP, 5-psid scanner, 23-psia reference pressure
$P2$	Flow angle pressure measured at Port 2 of 5-hole probe	ESP, 5-psid scanner, 23-psia reference pressure
$P3$	Flow angle pressure measured at Port 3 of 5-hole probe	ESP, 5-psid scanner, 23-psia reference pressure
$P4$	Flow angle pressure measured at Port 4 of 5-hole probe	ESP, 5-psid scanner, 23-psia reference pressure
$P5$	Flow angle pressure measured at Port 5 of 5-hole probe	ESP, 5-psid scanner, 23-psia reference pressure
$P6$	Static pressure measured by the static ring of 5-hole probe	ESP, 5-psid scanner, 23-psia reference pressure

TABLE IV. CRITICAL 5-HOLE FLOW ANGLE PROBE CALCULATED VARIABLES

Variable Name	Description	$f(x)$
$PAVG$	Average of Ports 2, 3, 4 and 5	$f(P2, P3, P4, P5)$
CA	Calibration pressure coefficient	$f(P1, P4, P5, PAVG)$
CB	Calibration pressure coefficient	$f(P1, P2, P3, PAVG)$
CM	Calibration pressure coefficient	$f(P1, PAVG)$
Co	Total pressure correction factor	$f(CA, CB, CM, Co_{model}))$

4.3 Temperature Calibration Instrumentation

4.3.1 2D RTD Array

Test section total temperature calibration data was collected using a two-dimensional (2D) RTD array, shown in Figure 6. The 2D RTD array is mounted to the walls, floor, and ceiling of the IRT test section just downstream of the center of the turntable. Figure 7 shows the numbering and position of each RTD relative to the floor and wind tunnel wall. The total temperature probes are 4-wire RTDs with a ceramic capsule sensor. Critical 2D RTD array measurements and calculated variables are shown in Table V.

Figure 6. 2D RTD array mounted in the IRT test section (forward looking aft).

Distance from Tunnel Floor, z [inches]	Distance from North Tunnel Wall, y [inches]						
	13.5	27	40.5	54	67.5	81	94.5
63	1	2	3	4	5	6	7
54	8	9	10	11	12	13	14
45	15	16	17	18	19	20	21
36	22	23	24	25	26	27	28
27	29	30	31	32	33	34	35
18	36	37	38	39	40	41	42
9	43	44	45	46	47	48	49

Figure 7. 2D RTD array layout.

TABLE V. 2D RTD ARRAY VARIABLES OF INTEREST

Variable Name	**Description**	$\boldsymbol{f(x)}$
$TTARRC(1-49)$	2D RTD array temperature neasurements	Accutech RTD
$ATTARRCC25$	Average of center 25 RTD array temperature measurements, thermal recovery corrected	$f(TTARCC, RTD_{models}, MTS)$
$TTDELTA$	Difference between average D-corner temperature and average corrected test section temperature	$f(TTDC, ATTARRCC25)$

5 Data Reduction

5.1 Overview

Figure 8 shows an overview of the components of an IRT calibration. The components are described in the following sections.

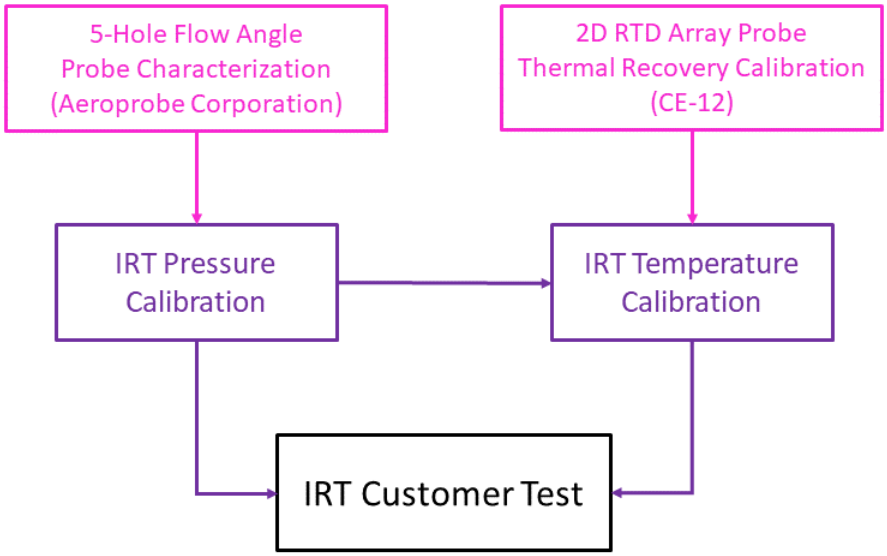

Figure 8. Overview of the IRT calibration process.

5.2 2D Array RTD Probe Thermal Recovery Calibration

Temperature probe measurements are affected by the air flowing over them. A thermal recovery factor for a temperature probe characterizes its ability to measure the true temperature of air as it moves across the probe tip. To quantify this effect, the 2D RTD array probes were calibrated in the NASA Glenn Research Center Free-Jet Probe Characterization Facility (CE–12). Curve fits representing thermal recovery factors as a function of Mach number were developed for each RTD probe. Figure 9 shows the test setup in CE-12. A flow chart of the 2D array probe calibration process is shown in Figure 10 and a list of critical 2D array probe calibration variables is shown in Table VI.

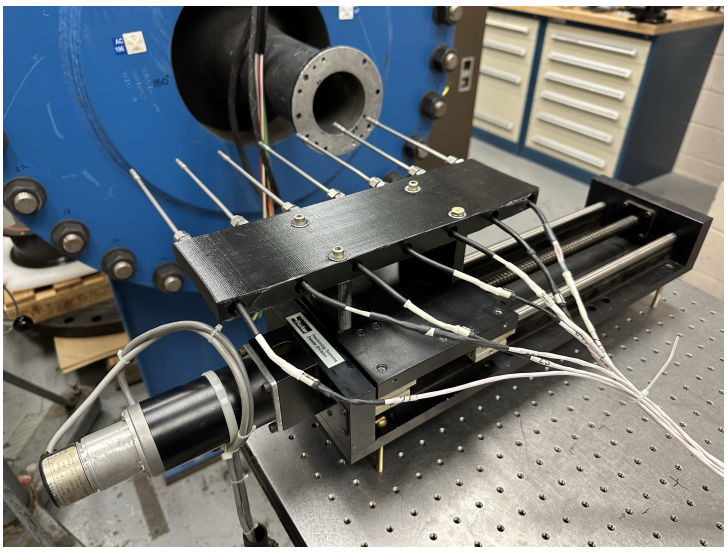

Figure 9. 2D RTD array probe thermal recovery calibration test setup.

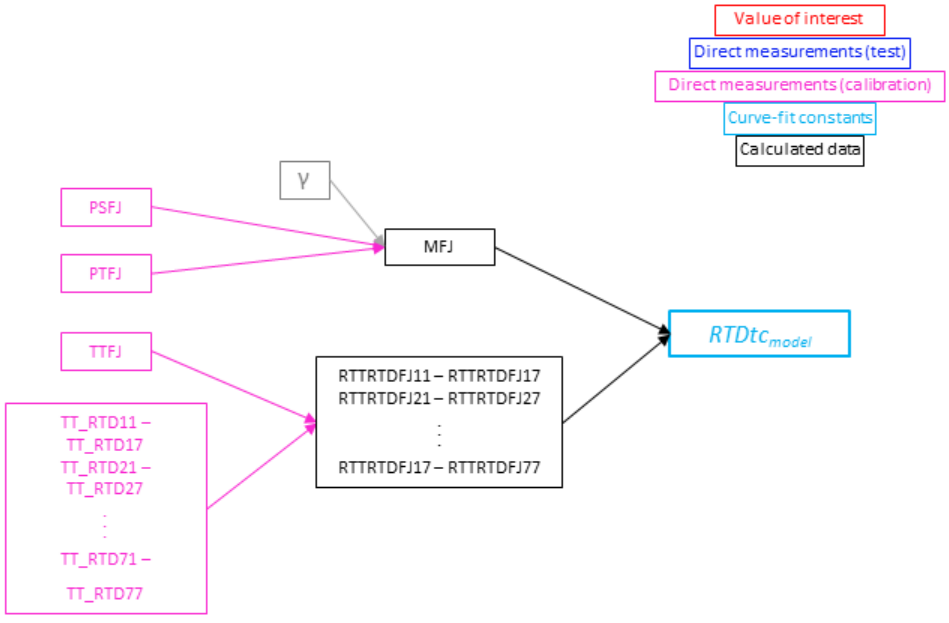

Figure 10. Data reduction flow chart for the 2D RTD array probe calibrations.

TABLE VI. CRITICAL 2D RTD PROBE CALIBRATION VARIABLES

Variable Name	**Description**	$\boldsymbol{f(x)}$
$PSFJ$	Free-jet static pressure	Measured
$PTFJ$	Free-jet total pressure	Measured
$TTFJ$	Free-jet total temperature	Measured
MFJ	Free-jet Mach number	$f(PSFJ, PTFJ)$
TT_RTD(11 to 77)	2D RTD array probe temperature	Measured
$RTTRTDFJ$(11 to 77)	Ratio of 2D RTD array probe temperature to free-jet total temperature	$f(TT\_RTD(11 \text{ to } 77), TTFJ)$

5.3 Aeroprobe 5-Hole Flow Angle Probe Characterization

Due to small variations in the manufacturing process, each 5-hole flow angle probe has slightly different aerothermal characteristics. Each probe is calibrated individually to develop a model (Co_{model}) to be used during testing to calculate a total pressure correction factor to be applied to measurements made by the probe. The 5-hole flow angle probe characterizations were performed at the Aeroprobe Corporation calibration facility. Figure 11 shows a flow chart of the Aeroprobe Corporation calibration process.

During calibration, Aeroprobe facility atmospheric and total pressures (Ps_{AP} and Pt_{AP}) and 5-hole flow angle probe port pressures ($P1_{AP}$ to $P6_{AP}$) are measured at a series of Mach number setpoints. Ps_{AP} is used as a reference pressure, which is combined with the other pressure measurements to obtain absolute pressures. $P1_{cal}$, PT_{cal}, and $PAVG_{cal}$ are used to calculate Co_{cal}. Coefficients CA_{cal}, CB_{cal}, and CM_{cal} are derived from $P1_{cal} - P5_{cal}$, PT_{cal}, and $PAVG_{cal}$. Co_{cal}, CA_{cal}, CB_{cal}, and CM_{cal} are used to derive a third-order curve fit model, Co_{model}, for each Mach number setpoint. Each 5-hole probe is calibrated independently and has its own set of characterization models for each Mach number setpoint. A list of critical 5-hole flow angle probe calibration variables is shown in Table VII.

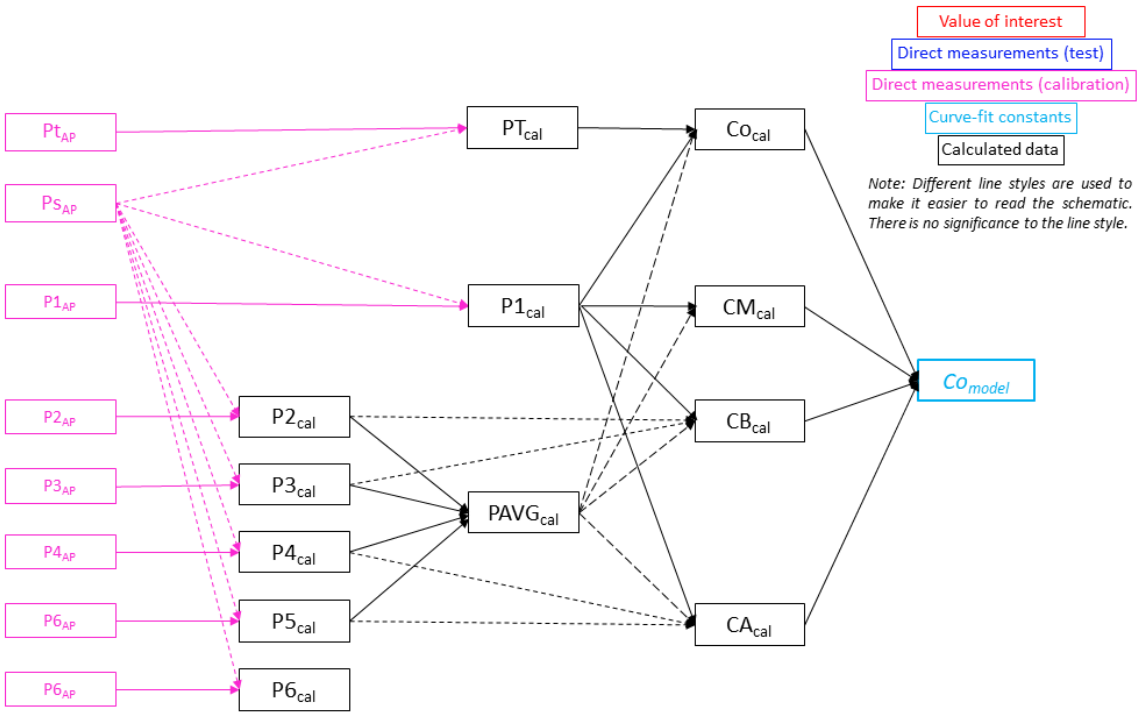

Figure 11. Data reduction flow chart for Aeroprobe Corporation 5-hole probe calibration.

TABLE VII. CRITICAL 5-HOLE PROBE CHARACTERIZATION VARIABLES

Variable Name	**Description**	$f(x)$
Ps_{AP}, Pt_{AP}	Aeroprobe facility atmospheric and total pressure	Measured
PT_{cal}	Aeroprobe facility test section total pressure	$f(Ps_{cal}, Pt_{cal})$
$P1_{cal}$	5-hole probe total pressure, Port 1	$f(Ps_{cal}, P1_{cal})$
$P2_{cal}$	5-hole probe flow angle pressure, Port 2	$f(Ps_{cal}, P2_{cal})$
$P3_{cal}$	5-hole probe flow angle pressure, Port 3	$f(Ps_{cal}, P3_{cal})$
$P4_{cal}$	5-hole probe flow angle pressure, Port 4	$f(Ps_{cal}, P4_{cal})$
$P5_{cal}$	5-hole probe flow angle pressure, Port 5	$f(Ps_{cal}, P5_{cal})$
$P6_{cal}$	5-hole probe static pressure, static ring	$f(Ps_{cal}, P6_{cal})$
$PAVG_{cal}$	Average of four angled pressure measurements	$f(P2_{cal}, P3_{cal}, P4_{cal}, P5_{cal})$
CA_{cal}	Calibration pressure coefficient	$f(P1_{cal}, P4_{cal}, P5_{cal}, PAVG_{cal})$
CB_{cal}	Calibration pressure coefficient	$f(P1_{cal}, P2_{cal}, P3_{cal}, PAVG_{cal})$
CM_{cal}	Calibration pressure coefficient	$f(P1_{cal}, PAVG_{cal})$
Co_{cal}	Calibration correction factor	$f(P1_{cal}, PT_{cal}))$
Co_{model}	Total pressure correction factor model	$f(CA_{cal}, CB_{cal}, CM_{cal})$

5.4 IRT Pressure Calibration

The purpose of the IRT pressure calibration is to develop curve fit models that relate test section pressure conditions to measured facility parameters. During the pressure calibration, the 6-ft quick-check rake is mounted in the IRT test section and fully populated with 11, 5-hole flow angularity probes. Pressure measurements from Ports $P1$ to $P5$ of the seven center-mounted probes, and the Co_{models} developed during the Aeroprobe Corporation calibration are used to find average corrected total pressure ($APTC$) in the test section. The average corrected static pressure ($APSC$) in the test section is assumed to be equal to the average of the static pressure measured at $P6$ of the seven center-mounted probes. Curve fit models relating $PTTS$ and $PSTS$ to IRT facility spray bar ($PAIRAVG$) and bellmouth ($PSBM$ and $PTBM$) pressure measurements are derived from the data. Figure 12 shows a flow chart of the pressure calibration data reduction process.

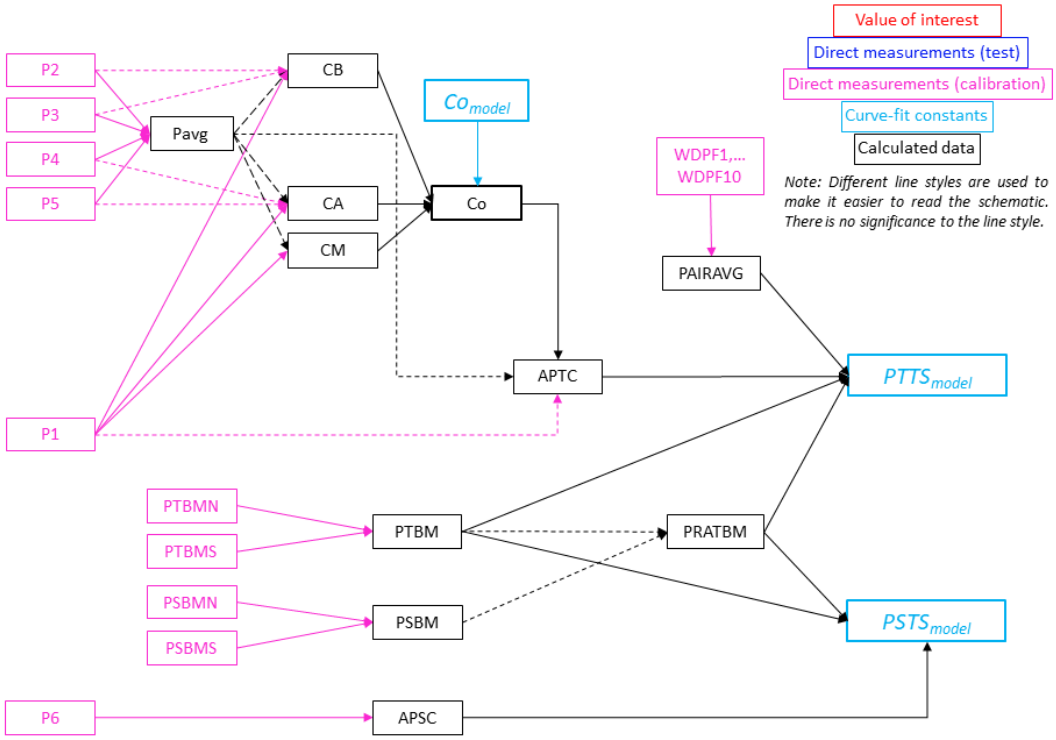

Figure 12. Data reduction flow chart for the IRT pressure calibration.

5.5 IRT Temperature Calibration

The purpose of the IRT temperature calibration is to develop curve fit models that relate test section total temperature conditions to measured facility parameters. During the temperature calibration, data was collected from facility instrumentation located in the D-corner ($TTDC$), bellmouth ($PSBM$ and $PTBM$) and at the spray bar manifolds ($PAIRAVG$). Test section temperature data ($TTARRC\_1$ to $TTARRC\_49$) was collected using the 2D RTD array described in Section 4.3.1.

$PSTS$ and $PTTS$ are calculated as a function of measured facility inputs and the curve fit models developed from the pressure calibration. Average corrected temperature in the test section ($ATTARRCC25$) is calculated from the core 25 2D RTD array measurements (see Figure 7), thermal recovery models developed from the RTD probe calibrations, and calculated test section Mach number (MTS). Curve fit models relating $TTTS$ to measured facility inputs were derived from the data.

It was determined that two separate curve fit models, $TTTS_{model(LowSpeed)}$, and $TTTS_{model(HighSpeed)}$ most accurately predicted test section temperature. The low speed model is applied for air speeds less than 50 knots, and the high speed model is applied for air speeds between 50 and 300 knots.

Figure 13 shows a flow chart of the temperature calibration data reduction process.

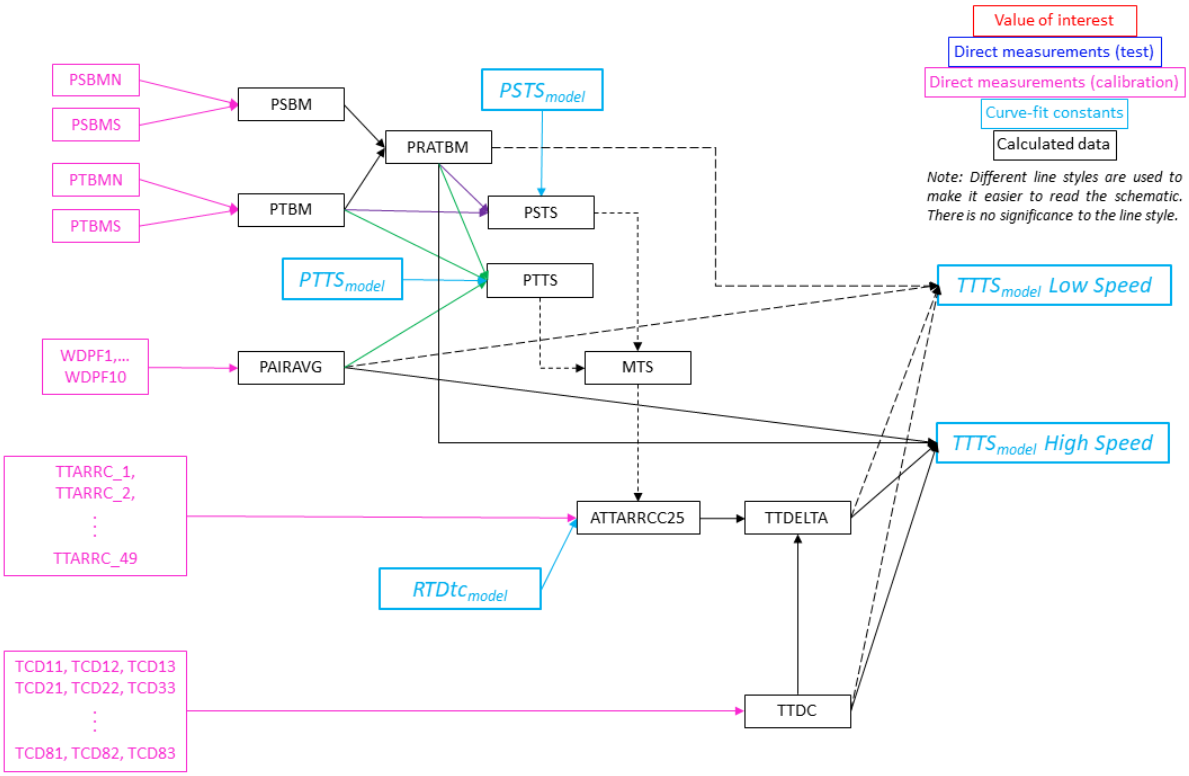

Figure 13. Data reduction flow chart for the IRT temperature calibration.

5.6 IRT Customer Test

During a customer test, facility data is collected from the D-corner, bellmouth and spray bar instrumentation ($TTDC$, $PSBM$, $PTBM$ and $PAIRAVG$, respectively). Test section pressures ($PSTS$ and $PTTS$) and test section total temperature ($TTTS$) are calculated using the facility measurements and the prediction models developed in the pressure and temperature calibrations. Test section VOIs, MTS, $TSTS$, and UTS are derived from $PSTS$, $PTTS$, and $TTTS$ as shown in Equations 1 through 3. The ratio of specific heats, γ, is assumed here to be a constant 1.4, and the universal gas constant, R, is assumed to be a constant 287.05 $N * m/(kg * kelvin)$.

Figure 14 shows a flow chart of the customer test data reduction process.

$$MTS = \sqrt{\frac{2}{\gamma - 1}\left[\left(\frac{PSTS}{PTTS}\right)^{-\frac{\gamma-1}{\gamma}} - 1\right]}, \tag{1}$$

$$TSTS = TTTS * (1 + \frac{\gamma - 1}{2} MTS^2), \tag{2}$$

$$UTS = MTS * \sqrt{\gamma * R * TSTS_{kelvin}}. \tag{3}$$

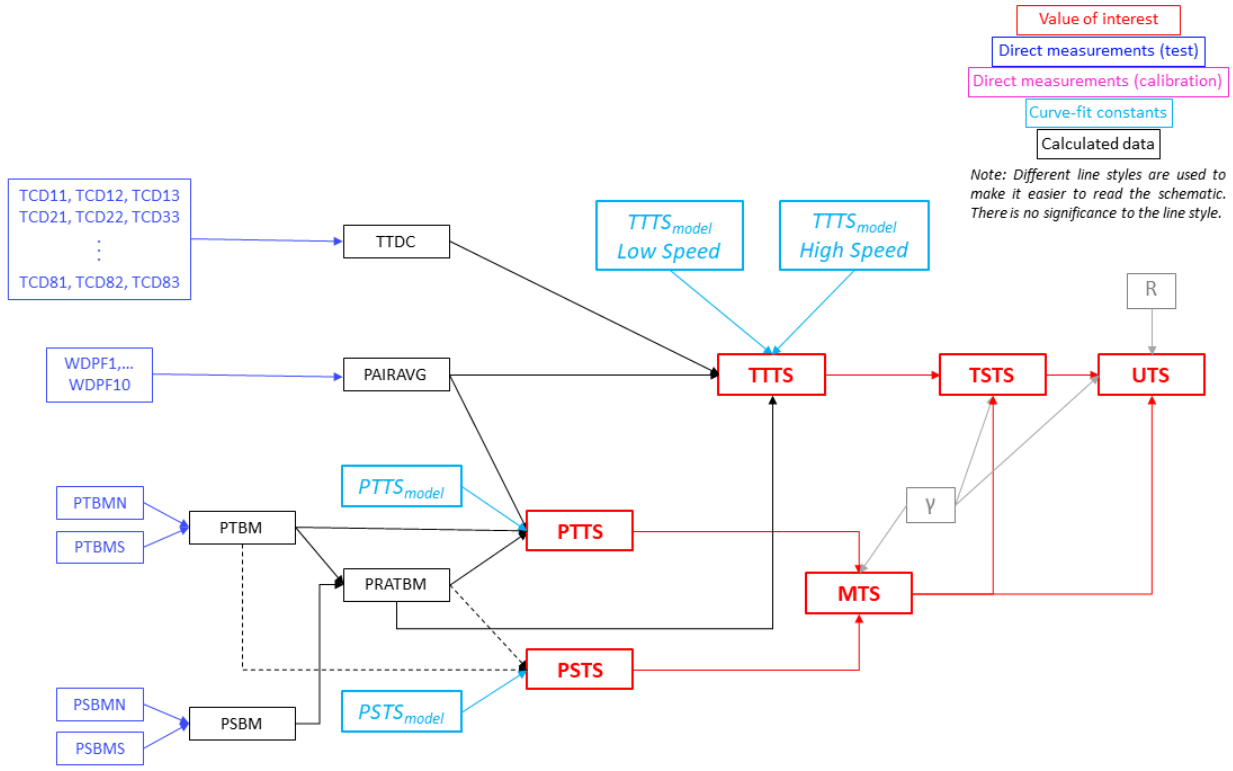

Figure 14. Data Reduction Flow Chart for an IRT Customer Test.

6 Uncertainty Analysis Overview and Methods

Following the classification scheme in the ASME and AIAA uncertainty standards and guides (Refs. [2] and [3]), uncertainty estimates are broken down into two main categories: random and systematic. This classification scheme helps to identify how the types of uncertainty can be best estimated and how they can be expected to affect data and subsequent calculations. Random uncertainty characterizes variation that is inherent to taking data in the real world. Environmental fluctuations, electrical noise, vibrations, variation in uncontrolled parameters, etc. are common sources of random uncertainty. Systematic uncertainty characterizes the biases that occur in measurements due to instrument behavior (non-linearity, hysteresis, etc.), instrument and model installation effects, data reduction choices, manufacturing quality, human operation, test procedures, etc. Systematic and random uncertainty results for the 2024 IRT calibration are addressed in this report.

Of note, during the early development of the Monte Carlo simulation model for the pressure calibration process, it was discovered that at airspeeds less than 25 knots, the errors introduced on the 5-hole probe port measurements may, in rare cases, result in a condition where the probe total pressure ($P1$) is nearly equal to the probe average pressure ($PAVG$). The difference of these variables ($P1 - PAVG$) appears in the denominator in calculations of the correction factor (Co). When this occurs, the resulting value for Co becomes abnormally large, which results in an unrealistic value of corrected total pressure, PTC. If this condition were to occur during an actual test, it would raise a flag to the staff that something was wrong and testing would be paused to investigate and address the issue. In a Monte Carlo simulation, the data reduction sequence is typically repeated 10,000 times. In this case, the 10,000-iteration simulation of the pressure calibration process was run three separate times. This anomaly occurred 0.1 percent of the time in one of the runs and was not observed in the other two runs. Because this condition occurred rarely in the Monte Carlo simulation, and that it would be considered invalid data during an actual test, these iterations were removed from the simulation data set when they occurred.

6.1 Systematic Uncertainty Analysis

Measurement uncertainties were propagated through a simulation of the data reduction sequences, discussed in Section 5, using the Monte Carlo Method (MCM) of uncertainty propagation. In brief, the MCM allows one to simulate tens of thousands of synthetic realizations of a test point, test matrix, or sequence of tests. As best as possible, the Monte Carlo simulation implements error population properly based on assumed error distributions, uncertainty correlations between measurements, and uncertainty correlations between test entries. Using uncertainty estimates, appropriate error populations are produced and added to associated measurements, simulating errors from known uncertainty sources. This produces large populations of perturbed measurements for all measurements taken during a test. Each set of perturbed measurements is then sent through the entire data reduction sequence to achieve thousands of simulated calculations of VOIs. The perturbed populations of the VOIs can then be analyzed to assess uncertainty in each variable.

The MCM was selected in lieu of the Taylor Series Method (TSM) due to the number of calculations involved and measurement uncertainty correlations present in the data reduction sequence. The method also lends itself well to quickly simulating theoretical changes for investigation of potential uncertainty improvements. For specific details on the methodology and application of both MCM and TSM, including examples of error population for uncorrelated and correlated uncertainties, consult References [4] and [5]).

6.2 Repeatability Uncertainty Analysis

Repeatability conceptually represents how consistently a measurement can be replicated. More technically, repeatability quantifies the level of variation observed in a parameter when a test point is repeated several times. The term is used interchangeably with random uncertainty throughout this document. This random variation can be assumed to follow a Gaussian or near-Gaussian distribution by the Central Limit Theorem (Ref. [4]), as it results from many different (and often indistinguishable) sources. It is therefore useful to define repeatability in relation to a common statistical parameter: the standard deviation of a population, sigma. This is a widely understood metric, as the 2-sigma value represents a 95 percent coverage interval about the population average in a Gaussian distributed population. Factors that contribute to random

uncertainty differ depending on the time scale over which the repeated measurements are obtained, making time scale a critical component to both quantifying and reporting repeatability. There are three distinct time scales that are useful to analyze: short-term (back-to-back or cyclic data), near-term (within-test or data taken over hours, days, or weeks), and long-term (between-test or data taken over months or years). Each of these time scales captures a different scope of variability. Short-term repeatability captures variation at the instrument level, near-term repeatability captures variation at the facility level, while long-term repeatability captures variation at the process level. Figure 15 lists some of the factors given that impact variability for these time scales. In general, the level of variation increases as the time scale increases because more sources of variation tend to become influential as time passes.

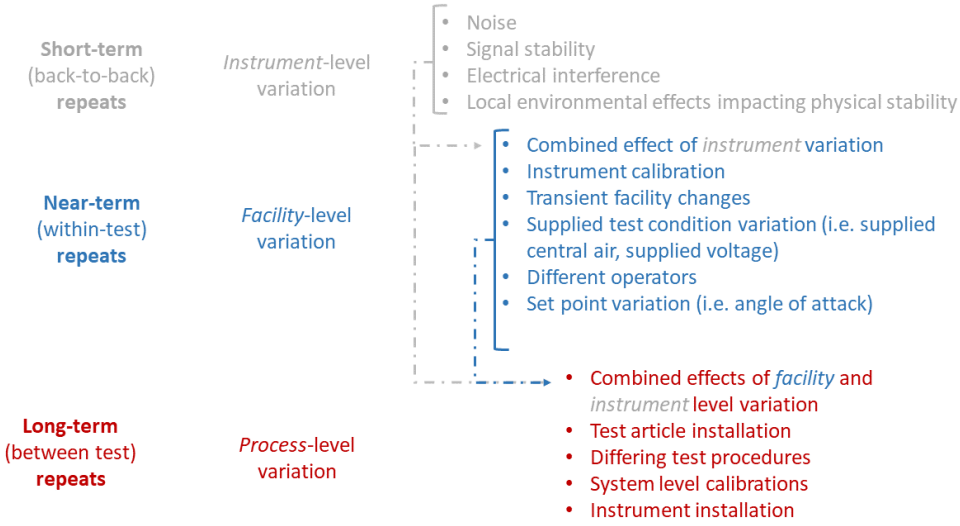

Figure 15. Factors impacting repeatability at different time scales.

Random uncertainty was quantified for the 2024 Characterization Test as between-test, (i.e., in a long-term time scale). Calibration data collected over four years (2021, 2023, 2024 and 2025) were used in this analysis. As a starting hypothesis, it was assumed that the random uncertainty in the VOIs may be represented by the RMSE of the prediction models developed for $PSTS$, $PTTS$, and $TTTS$ during the calibration process, and that there is no additional random uncertainty. To test this hypothesis, a statistical analysis comparing the predicted value of the VOIs to the mean of the four years of calibration data for the VOIs was performed. The results showed that the difference between the predicted and mean values of the VOIs was not statistically signficant. The conclusion is that the RMSE of the prediction models is a good estimate of the random uncertainty and that they do not contain a bias offset.

6.3 Elemental Standard Uncertainty Estimates

An elemental standard uncertainty is defined as "an estimate of the standard deviation of the parent population from which a particular elemental error originates." (See the ISO *Guide to the Expression of Uncertainty in Measurement* (Ref. [6]) and Coleman and Steele (Ref. [4]).) All elemental standard uncertainty estimates, sources, and quantities that serve as inputs into the error propagation are detailed in this section. Elemental standard uncertainty estimates for measurement x will be denoted as b_x following standard nomenclature for systematic standard uncertainty categorization. Unless otherwise noted, a normal distribution of errors is assumed for elemental uncertainties propagated. Calibration cycles of all instruments involved in the data reduction are considered and accounted for within the simulations. The specific heat ratio for air, γ, as well as gas constants used in the data reduction scheme are assumed to have negligible uncertainty contributions.

Elemental uncertainties are estimated on a source-by-source basis. The TSM for uncertainty propagation is employed by MANTUS (Measurement Analysis Tool for Uncertainty in Systems) (Refs. [5] and [7], to be published), an Excel® based tool that allows the user to break down the overall measurement into component parts, or modules, to easily handle the analysis of multilevel instrumentation systems. This captures instrument chain uncertainty contributions from the point of measurement through the data system output as depicted in Figure 16.

Systematic uncertainty related to the accuracy of measurements and measurement systems was estimated using the MANTUS tool. Unless otherwise stated, elemental uncertainty estimates represent a standard, 1-sigma, uncertainty value and are assumed to be characterized by a normal distribution.

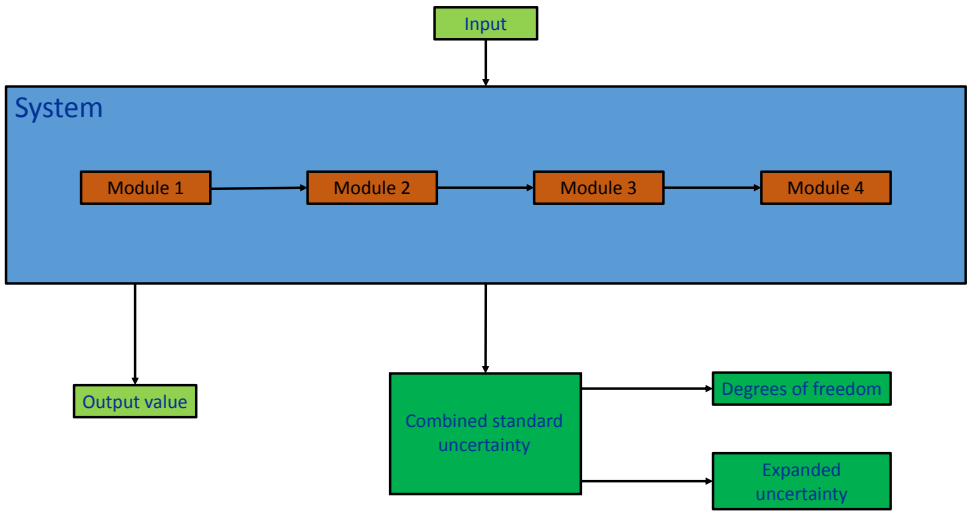

Figure 16. Instrumentation-level uncertainty analysis flow.

6.3.1 5-Hole Flow Angle Probe Characterization Elemental Uncertainty Estimates

Elemental uncertainty estimates for all critical measurements required to calculate the 5-hole flow angle probe calibration VOIs are listed in Table VIII.

TABLE VIII. ELEMENTAL UNCERTAINTY ESTIMATES FOR THE 5-HOLE PROBE CHARACTERIZATION

Measurement system description	Calibration velocity	Label	Uncertainty estimate	Units
Pressure transducer, ±4 inches H_2O	Mach 0.036	b_{M036}	0.0019	Torr
Pressure transducer, ±4 inches H_2O	Mach 0.08	b_{M080}	0.0019	Torr
Pressure transducer, ±10 inches H_2O	Mach 0.15	b_{M150}	0.0047	Torr
Pressure transducer, ±2 psi	Mach 0.23	b_{M230}	0.0259	Torr
Pressure transducer, ±2 psi	Mach 0.30	b_{M300}	0.0259	Torr
Pressure transducer, ±5 psi	Mach 0.38	b_{M380}	0.0646	Torr
Pressure transducer, ±5 psi	Mach 0.45	b_{M450}	0.0646	Torr
Pressure transducer, ±5 psi	Mach 0.55	b_{M550}	0.0646	Torr
Reference pressure transducer, 15 psi	———	b_{Ps}	0.5818	Torr

6.3.2 2D RTD Array Probe Calibration Elemental Uncertainty Estimates

Elemental uncertainty estimates for all critical measurements required to calculate the 2D RTD array probe calibration VOIs are listed in Table IX.

TABLE IX. ELEMENTAL UNCERTAINTY ESTIMATES FOR THE 2D RTD ARRAY PROBE CALIBRATION

Measurement system description	Label	Uncertainty estimate	Units
Mensor CPG2500 pressure transmitter, 0 to 17 psia	b_{PS}	0.0008	psia
Mensor CPG2500 pressure transmitter, 0 to 27 psia	b_{PT}	0.0012	psia
Omega PR-25AP-1/10 RTD probe	b_{TT}	See Figure 17	°F
Accutech AI-1500 RTD	$b_{rtdArray}$	0.126	°F

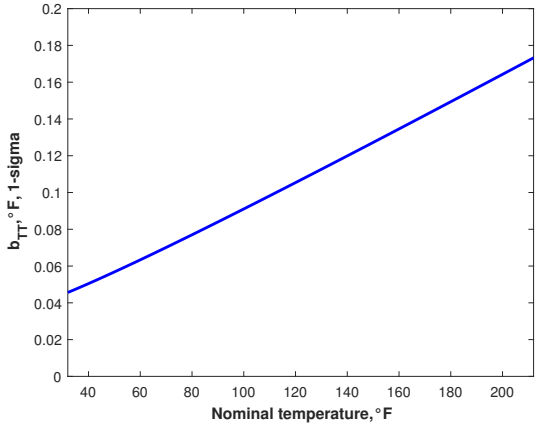

Figure 17. Elemental uncertainty estimates for Omega PR-25AP-1/10 RTD instrumentation.

6.3.3 IRT Facility Calibration Elemental Uncertainty Estimates

Elemental uncertainty estimates for all critical measurements required to calculate the facility VOIs are listed in Table X.

TABLE X. ELEMENTAL UNCERTAINTY ESTIMATES FOR THE IRT FACILITY CALIBRATION

Measurement system description	Label	Uncertainty estimate	Units
Netscanner ESP PCU, 0 to 23 psia	b_{Pref}	0.0017	psia
Netscanner 9816 module, ±5-psid	b_{NS9816_5psid}	0.0025	psid
Honeywell FPG transducer, 0 to 100 psig	$b_{HW\_FPG\_100psig}$	0.0651	psig
Accutech AI-1500 RTD	$b_{AccutechRTD}$	0.07	°C
Omega PT-100AA RTD probe	$b_{DcornerRTD}$	See Figure 18	°C

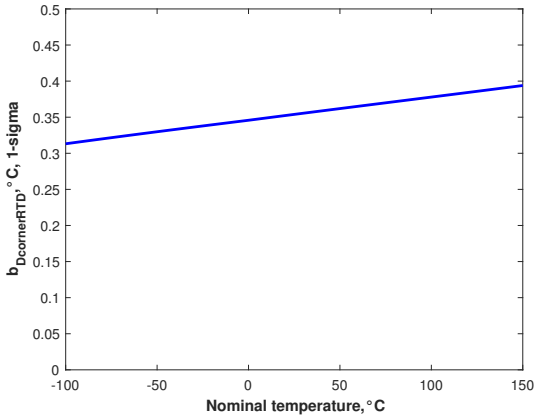

Figure 18. Elemental uncertainty estimates for D-corner RTD instrumentation.

6.3.4 Prediction Model Elemental Uncertainty Estimates

For any test-derived regression model, two uncertainty sources must be considered: the uncertainty fossilized into the model due to uncertainties present in the data obtained during the characterization test and the uncertainty due to the residual error of the model selected. The former of these is inherent in the results of the MCM because the characterization tests are included in the cascading simulation; the latter requires statistical analysis of the regression model residuals. If the residuals are normally distributed, independent, and have a constant variance, the Root Mean Square Error (RMSE) of the curve fit can be used as the prediction model regression uncertainty estimate. The IRT calibration curves meet this criteria. The prediction model regression uncertainty estimates for curve fit model x will be denoted as s_x. They are listed in Table XI.

TABLE XI. PREDICTION MODEL UNCERTAINTY ESTIMATES

Uncertainty Label	Uncertainty Estimate
$s_{Co\ RMSE\ P1}$	0.0024
$s_{Co\ RMSE\ P2}$	0.0017
$s_{Co\ RMSE\ P3}$	0.0031
$s_{Co\ RMSE\ P4}$	0.0024
$s_{Co\ RMSE\ P5}$	0.0023
$s_{Co\ RMSE\ P6}$	0.0033
$s_{Co\ RMSE\ P7}$	0.0027
$s_{Co\ RMSE\ P8}$	0.0021
$s_{Co\ RMSE\ P9}$	0.0029
$s_{Co\ RMSE\ P10}$	0.0014
$s_{Co\ RMSE\ P11}$	0.0018
$s_{Co\ RMSE\ P12}$	0.0018
$s_{Co\ RMSE\ P13}$	0.0045
$s_{Co\ RMSE\ P14}$	0.0033
$s_{RTD\ RMSE}$	0.0002
$s_{PS\ RMSE}$	0.00002
$s_{PT\ RMSE}$	0.00003
$s_{TT\ High\ RMSE}$	0.137
$s_{TT\ Low\ RMSE}$	0.129

7 Results

The results presented here are from the 6- by 9-Foot IRT 2024 calibration measurement uncertainty analysis. Results are presented as expanded uncertainties, with a coverage factor of $k = 2$, which is approximately equal to a level of confidence of 95 percent. The expanded uncertainties are denoted by B_x for systematic uncertainty. Each VOI is treated as univariate.

Uncertainty Percent Contribution (UPC) charts, which show the primary factors contributing to the overall uncertainty in a VOI and the percentage that each factor contributes, are presented for the systematic uncertainty of the calculated VOIs. The charts show only those factors that contribute greater than 1 percent to the total uncertainty.

The results presented here include the characterization of systematic effects from instrumentation and prediction models.

7.1 Test Section Static and Total Pressure

The uncertainties associated with test section static pressure (B_{PSTS}) and test section total pressure (B_{PTTS}) are shown in Figures 19 and 20, respectively. Uncertainty in test section pressure is unaffected by spray bar air pressure. B_{PSTS} shows a slight, linearly positive trend with respect to test section Mach number (MTS) and B_{PTTS} shows a quadratic relationship to MTS. Formulas for predicting B_{PSTS} and B_{PTTS} are shown in the figures; however, both may be reasonably represented by the constant values summarized in Table XII.

TABLE XII. EXPANDED SYSTEMATIC UNCERTAINTY IN TEST SECTION PRESSURE

Variable Name	Uncertainty [psi]
$PSTS$	5.5×10^{-3}
$PTTS$	6.2×10^{-3}

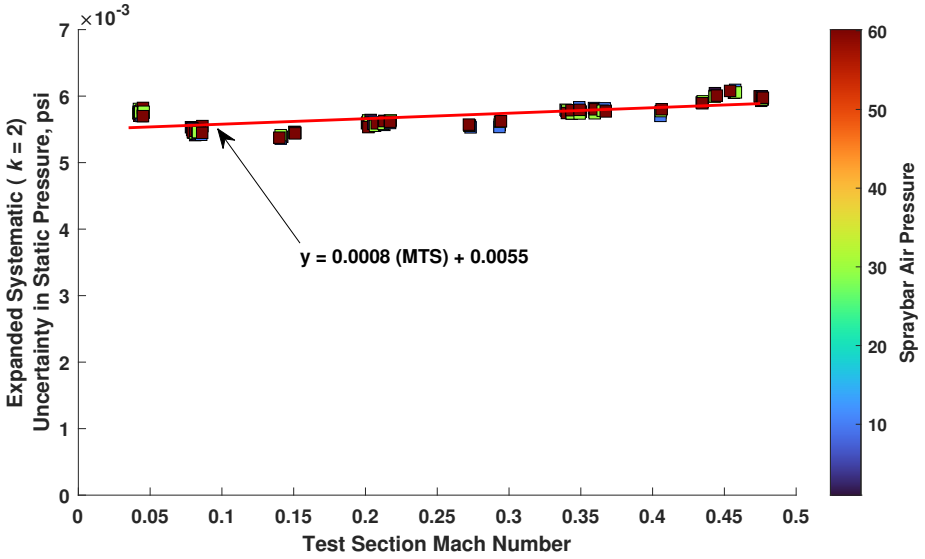

Figure 19. Expanded systematic uncertainty in $PSTS$.

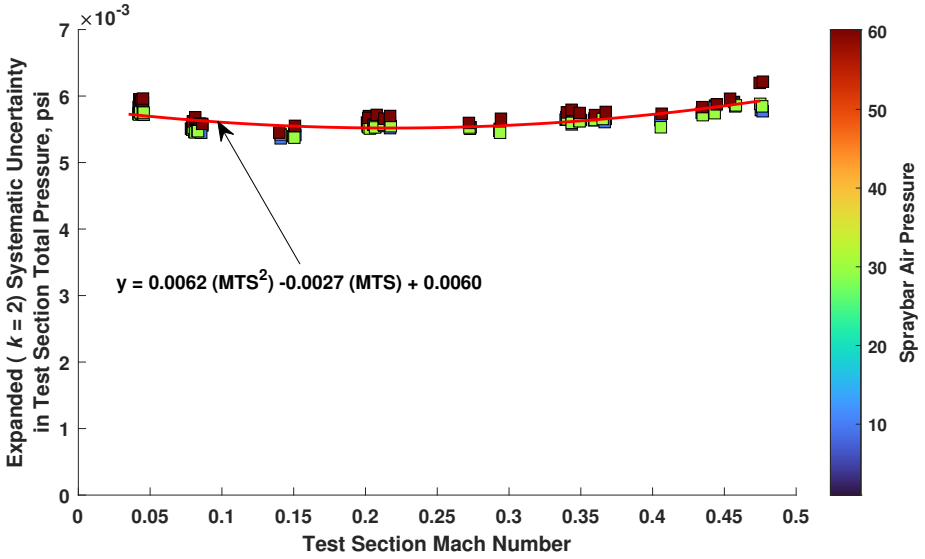

Figure 20. Expanded systematic uncertainty in $PTTS$.

UPC charts for B_{PSTS} and B_{PTTS} are shown in Figure 21. UPC distributions for B_{PSTS} and B_{PTTS} are uniform throughout the operating envelope. In both cases, the bellmouth reference pressure ($ESPREF$) accounts for about 36 percent of the uncertainty and the pressure calibration process accounts for 24 to 26 percent. The remaining uncertainty contribution may be attributed to the bellmouth static pressure ($PSBM$) for B_{PSTS} and bellmouth total pressure ($PTBM$) for B_{PTTS}.

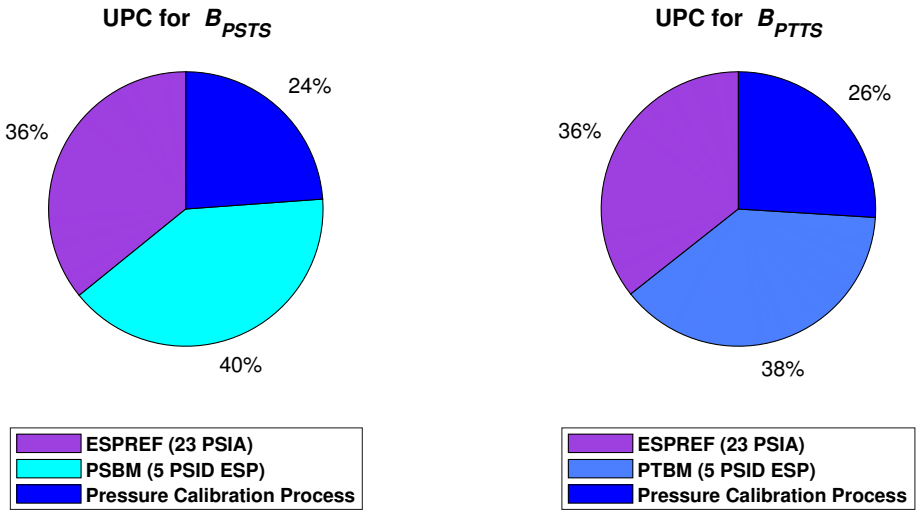

Figure 21. Uncertainty percent contributions for $PSTS$ and $PTTS$.

7.2 Test Section Total Temperature (TTTS)

Low airspeeds (<50 knots). Figure 22 shows the uncertainty in $TTTS$ (B_{TTTS}) at low airspeeds. At less than 50 knots, B_{TTTS} is affected by the spray bar air pressure ($PAIRAVG$). Formulas representing the trendlines for predicting B_{TTTS} at specific spray bar settings are shown in Figure 22; however, B_{TTTS}, at low airspeeds, may also be represented by the constant values summarized in Table XIII.

TABLE XIII. EXPANDED SYSTEMATIC UNCERTAINTY IN *TTTS* AT LOW AIRSPEEDS

PAIRAVG Setpoint	Uncertainty [°C]
1 psi	0.31
10 psi	0.31
30 psi	0.33
60 psi	0.37

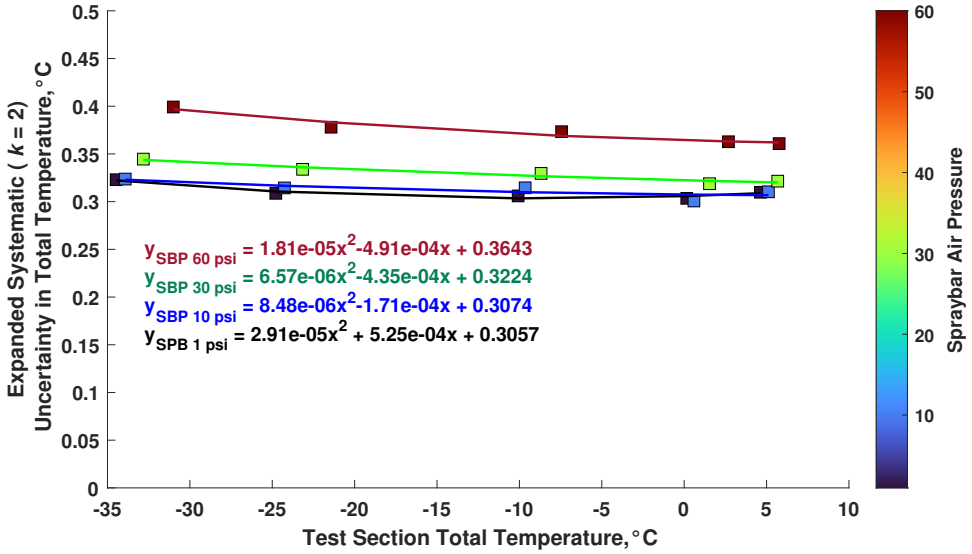

Figure 22. Expanded systematic uncertainty in *TTTS*, at low airspeeds.

High airspeeds (between 50 and 300 knots). Figure 23 shows the uncertainty in $TTTS$ (B_{TTTS}) at high airspeeds. B_{TTTS} is constant and minimally affected by $PAIRAVG$ in this operating range. A value of ±0.32 °C represents a conservative estimate for B_{TTTS} that encompasses the Monte Carlo simulation results in this airspeed range.

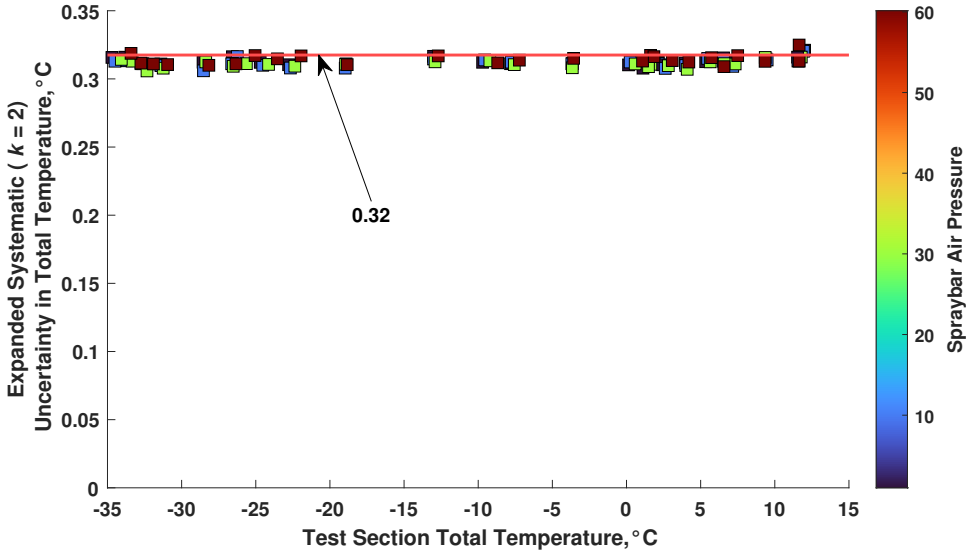

Figure 23. Expanded systematic uncertainty in *TTTS* at high airspeeds.

Uncertainty percent contributions, low and high airspeeds. Figure 24 shows UPC charts for B_{TTTS} as a function of $PAIRAVG$ and airspeed. At airspeeds less than 50 knots, the root mean square error of the temperature calibration models ($RMSE - TemperatureModel$) is the dominant contributor to B_{TTTS}. Consistent contributions from D-corner RTD temperature measurements ($TTDC$) and the temperature calibration process are present at all spray bar pressure settings. Significant contributions from $PSBM$ and $PTBM$ are introduced, and increase, as $PAIRAVG$ increases.

From 50 to 300 knots, $TTTS$ UPC distributions are unaffected by $PAIRAVG$. $RMSE-TemperatureModel$ is the dominant contributor to B_{TTTS} along with contributions from $TTDC$ and the temperature calibration process.

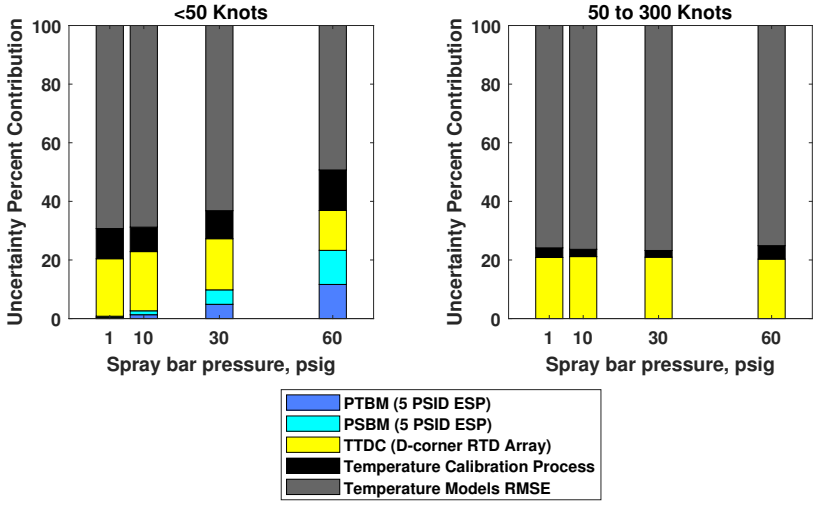

Figure 24. Uncertainty percent contributions for *TTTS*.

7.3 Test Section Static Temperature (TSTS)

Figure 25 shows the uncertainty in $TSTS$ (B_{TSTS}) at low airspeeds (<50 knots) and Figure 26 shows B_{TSTS} at high airspeeds (between 50 and 300 knots). B_{TSTS} behaves similarly to that seen for B_{TTTS}. Formulas representing the trendlines for predicting B_{TSTS} at low airspeeds are shown in Figure 26; however, B_{TSTS}, at low airspeeds, may also be represented by the constant values summarized in Table XIV. At airspeeds between 50 and 300 knots, B_{TSTS} is represented by a value of ±0.32 °C.

TABLE XIV. EXPANDED SYSTEMATIC UNCERTAINTY IN *TSTS* AT LOW AIRSPEEDS

PAIRAVG Setpoint	Uncertainty [°C]
1 psi	0.32
10 psi	0.32
30 psi	0.34
60 psi	0.38

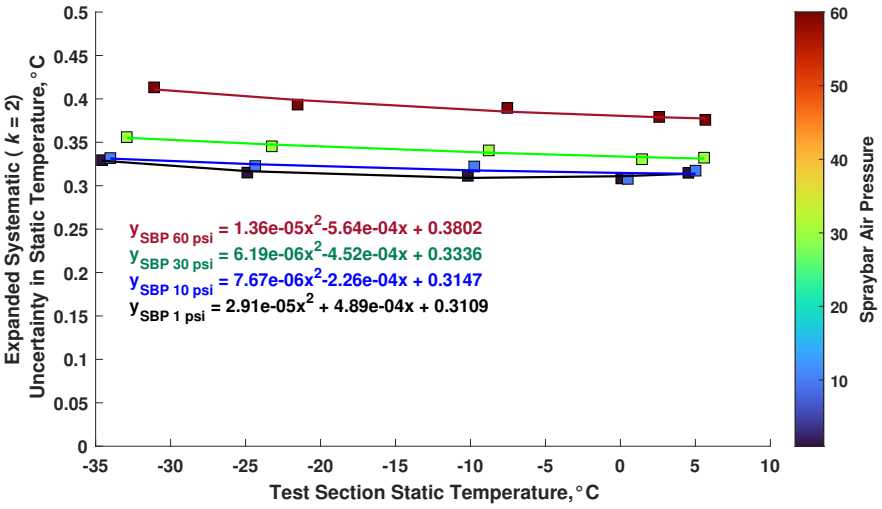

Figure 25. Expanded systematic uncertainty in *TSTS* at low airspeeds.

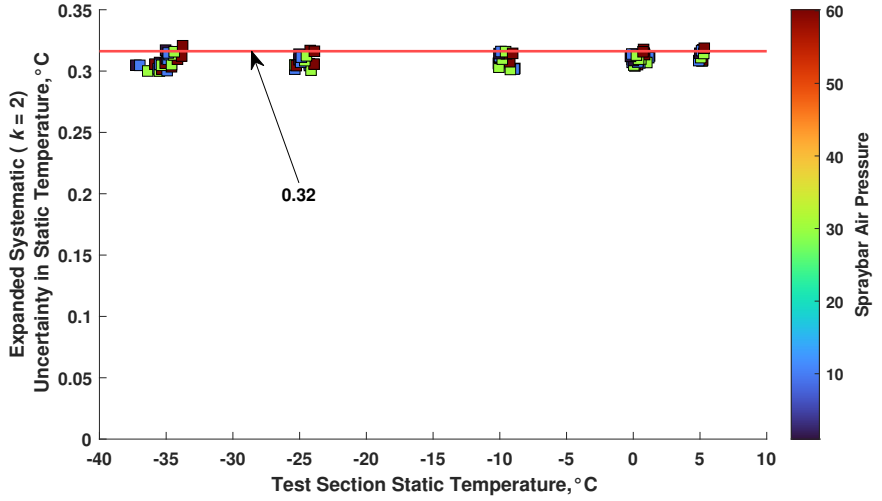

Figure 26. Expanded systematic uncertainty in *TSTS* at high airspeeds.

UPC charts for B_{TSTS} are shown as a function of $PAIRAVG$ and airspeed in Figure 27. At airspeeds less than 50 knots, $RMSE - TemperatureModel$ is the dominant contributor to B_{TSTS} with consistent contributions from $TTDC$ and the temperature calibration process at all spray bar pressure settings. At low airspeeds, signficant contributions from $PSBM$ and $PTBM$ are introduced, and increase, as $PAIRAVG$ increases.

From 50 to 300 knots, UPC distributions for B_{TSTS} are unaffected by $PAIRAVG$. The dominant contributor to B_{TSTS} is $RMSE - TemperatureModels$ along with contributions from $TTDC$ and the temperature calibration process.

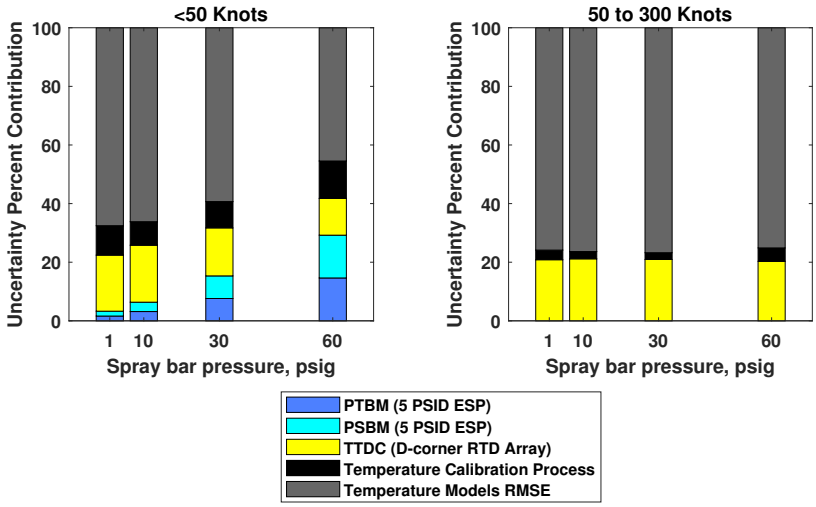

Figure 27. Uncertainty percent contributions for $TSTS$.

7.4 Test Section Mach Number (MTS) and Airspeed (UTS)

Figures 28 and 29 show the uncertainty in MTS (B_{MTS}) and UTS (B_{UTS}), respectively. Formulas respresenting the trendlines for these VOIs are shown in Table XV. B_{MTS} and B_{UTS} are minimally affected by $PAIRAVG$. Both decrease asymptotically as the tunnel airspeed increases and rise sharply below 100 knots. This sharp rise in uncertainty is mostly due the fact that calculations MTS and UTS are dependent on calculated pressures $PSTS$ and $PTTS$ (see Section 5.6). At low airspeeds, static and total pressure are very nearly the same, so small errors in these variables may result in larger uncertainties when propagated through the data reduction using MCM.

TABLE XV. FORMULAS FOR EXPANDED SYSTEMATIC UNCERTAINTY IN *MTS* AND *UTS*

Variable Name	Uncertainty Formula
MTS	$0.0002 \times MTS^{-1.2160} + 0.0004$
UTS	$284.05 \times UTS^{-1.2416} + 0.2917$

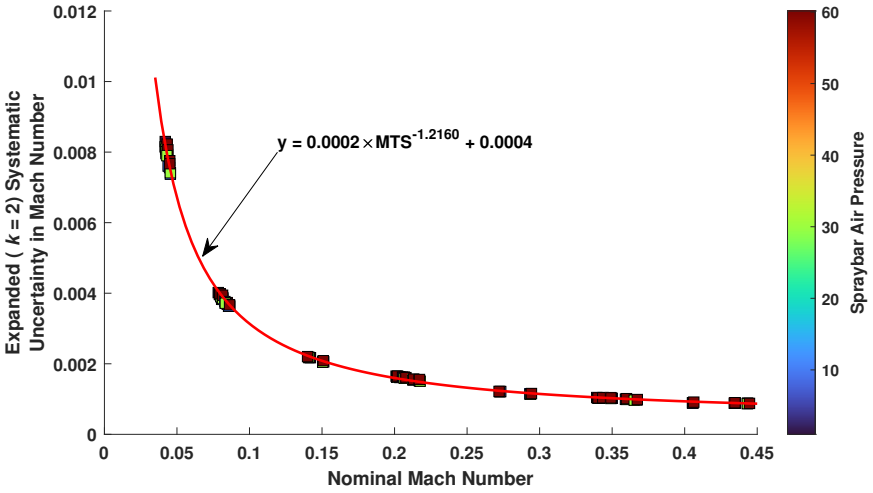

Figure 28. Expanded systematic uncertainty in *MTS*.

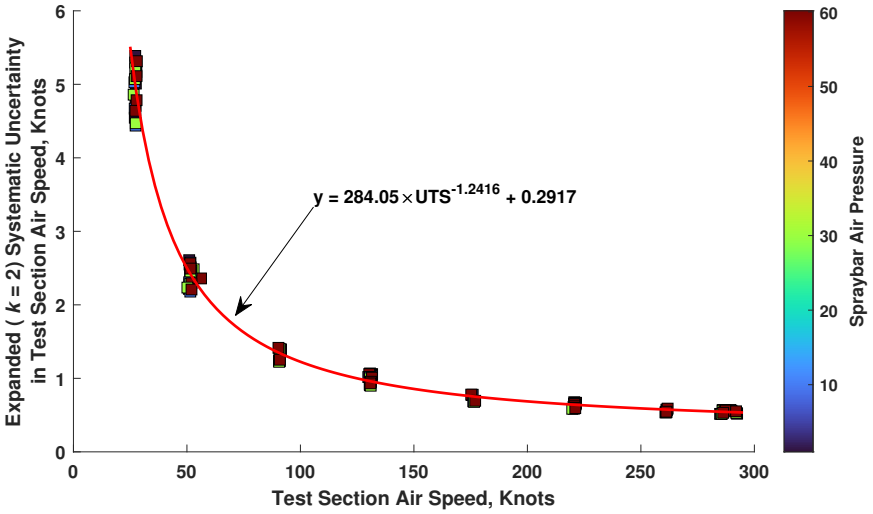

Figure 29. Expanded systematic uncertainty in *UTS*.

Figure 30 shows a UPC chart for B_{MTS}. UPC profiles for B_{MTS} are uniform throughout the operating envelope. The primary contributors to B_{MTS} are $PSBM$, $PTBM$ and the pressure calibration process.

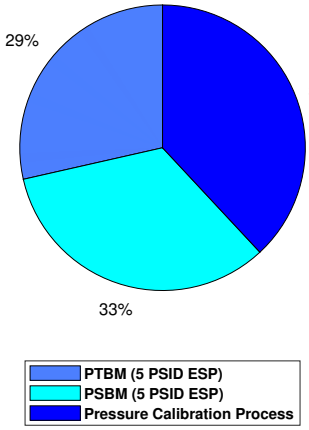

Figure 30. Uncertainty percent contributions for *MTS*.

Figure 31 shows UPC charts for B_{UTS} as a function of airspeed. UPC profiles of B_{UTS} are unaffected by spray bar air pressure but are affected by airspeed. $PSBM$, $PTBM$, and the pressure calibration process are the dominant contributors to B_{UTS} throughout the operating range of the IRT (25 to 300 knots). A small contribution from $RMSE - TemperatureModel$ appears at 90 knots and increases as airspeed is increased. Contributions from $TTDC$ and the temperature calibration process appear at 130 knots and increase as airspeed increases.

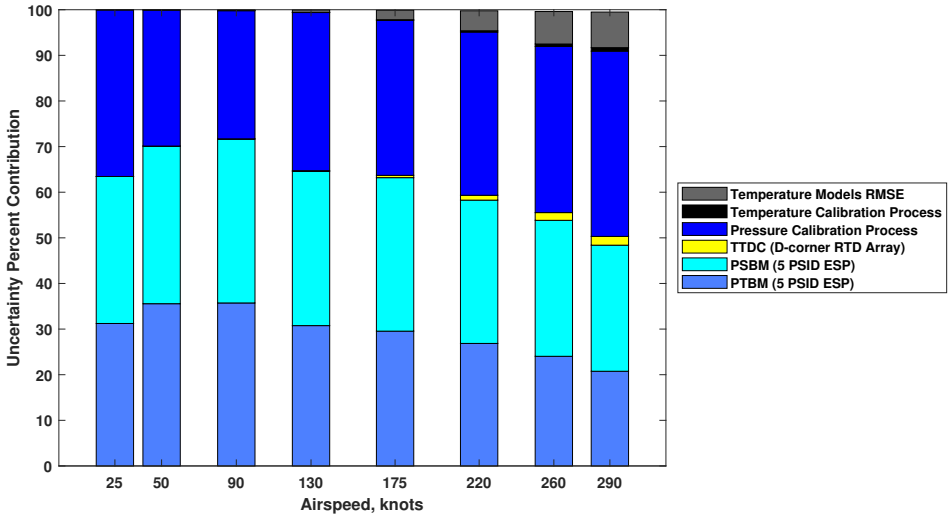

Figure 31. Uncertainty percent contributions for *UTS*.

8 Conclusions

Uncertainty in the 6- by 9-Foot IRT was characterized by modeling the expanded systematic uncertainty in the VOIs using the Monte Carlo method of uncertainty propagation. The random uncertainty in the VOIs is captured in the RMSE of the prediction models. Analysis of the MUA simulation results shows that the characterization models, instrumentation measurements, and facility operating setpoints affect the uncertainty in the VOIs differently depending upon the VOI. The results, summarized in Table XVI are within expected limits.

TABLE XVI. SUMMARY OF MUA RESULTS WITH 95 PERCENT LEVEL OF CONFIDENCE

Test Section VOI	**Uncertainty Range**
Static pressure	0.006 psi
Total pressure	0.006 psi
Total temperature	0.31 to 0.37 °C
Static temperature	0.32 to 0.38 °C
Mach number	0.001 to 0.008
Airspeed	0.5 to 5.4 knots

References

1. Parsons, E. & Johnson, A. M.: Full Aerothermal Characterization of the NASA Glenn Research Center 6- by 9-Foot Icing Research Wind Tunnel (2023 and 2024 Tests). Calibration Report (National Aeronautics and Space Administration, to be published).
2. American Society of Mechanical Engineers: Test Uncertainty. Standard ASME PTC 19.1-2013 (2014).
3. American Institute of Aeronautics and Astronautics: Assessment of Experimental Uncertainty with Application to Wind Tunnel Testing. Standard AIAA S-071A-1999 (1999).
4. Coleman, H. W. & Steele, W. G.: Experimentation, Validation and Uncertainty Analysis for Engineers Third Edition (John Wiley and Sons, Inc., 2009).
5. Stephens, J., Hubbard, E., Walter, J., *et al.:* Uncertainty Analysis of the NASA Glenn 8×6 Supersonic Wind Tunnel. Contractor Report NASA/CR-2016-219411 (National Aeronautics and Space Administration, 2016).
6. Joint Committee for Guides in Metrology: Evaluation of Measurement Data – Guide to the Expression of Uncertainty in Measurement. Guide JCGM 100:2008 (International Organization for Standardization, 2008).
7. Rouse, B., Morales, J. & McElroy, J.: Measurement Analysis Tool for Uncertainty in Systems Overview. Contractor Report (National Aeronautics and Space Administration, to be published).